Journal of Bioscience and Bioengineering
VOL. 135 No. 6, 493–499, 2023

www.elsevier.com/locate/jbiosc

Microfluidic encapsulation of photosynthetic cyanobacteria in hydrogel microparticles augments oxygen delivery to rescue ischemic myocardium

Lyndsay Mariah Stapleton,[1,2] Justin Michael Farry,[2] Yuanjia Zhu,[1,2] Haley Joan Lucian,[2] Hanjay Wang,[2] Michael John Paulsen,[2] Kailey Pearl Totherow,[1] Gillie Agmon Roth,[1] Kara Kimberly Brower,[1] Polly Morrell Fordyce,[1,3,4,5] Eric Andrew Appel,[1,6] and Yi-Ping Joseph Woo[1,2,*]

Department of Bioengineering, Stanford University, Stanford, CA 94305, USA,[1] Department of Cardiothoracic Surgery, Stanford University, Stanford, CA 94305, USA,[2] Department of Genetics, Stanford University, Stanford, CA 94305, USA,[3] ChEM-H Institute, Stanford University, Stanford, CA 94305, USA,[4] Chan Zuckerberg Biohub, San Francisco, CA 94110, USA,[5] and Department of Materials Science & Engineering, Stanford University, Stanford, CA 94305, USA[6]

Received 19 October 2022; accepted 2 March 2023
Available online 23 March 2023

Cardiovascular disease, primarily caused by coronary artery disease, is the leading cause of death in the United States. While standard clinical interventions have improved patient outcomes, mortality rates associated with eventual heart failure still represent a clinical challenge. Macrorevascularization techniques inadequately address the microvascular perfusion deficits that persist beyond primary and secondary interventions. In this work, we investigate a photosynthetic oxygen delivery system that rescues the myocardium following acute ischemia. Using a simple microfluidic system, we encapsulated *Synechococcus elongatus* into alginate hydrogel microparticles (HMPs), which photosynthetically deliver oxygen to ischemic tissue in the absence of blood flow. We demonstrate that HMPs improve the viability of *S. elongatus* during the injection process and allow for simple oxygen diffusion. Adult male Wistar rats (n = 45) underwent sham surgery, acute ischemia reperfusion surgery, or a chronic ischemia reperfusion surgery, followed by injection of phosphate buffered saline (PBS), *S. elongatus* suspended in PBS, HMPs, or *S. elongatus* encapsulated in HMPs. Treatment with *S. elongatus*-HMPs mitigated cellular apoptosis and improved left ventricular function. Thus, delivery of *S. elongatus* encapsulated in HMPs improves clinical translation by utilizing a minimally invasive delivery platform that improves *S. elongatus* viability and enhances the therapeutic benefit of a novel photosynthetic system for the treatment of myocardial ischemia.

[**Key words:** Hydrogel; Microparticles; Ischemia reperfusion; Microfluidics; Oxygen delivery]

Cardiovascular disease continues to be the leading cause of death in the United States (US), with 15.5 million Americans currently suffering from coronary artery disease (1) and 6.2 million experiencing heart failure (2). The US spends nearly $32 B dollars on the treatment of heart failure, including direct healthcare services, medications, and work absences (3). Current treatment of severe coronary disease and acute myocardial infarction typically relies on reperfusion therapies, including fibrinolytic therapy, percutaneous coronary intervention, and coronary artery bypass grafting. These methods, while successful at restoring macrovascular blood flow after infarction, exhibit high in-hospital mortality rates (5–6%) and one-year mortality rates (7–18%) (4). They also fail to address microvascular perfusion deficits resulting in cardiomyocyte death, downstream ventricular remodeling, progression to heart failure, and early mortality (5). Promising alternatives and combinatorial approaches such as biomaterial therapy, with and without therapeutic cargo, have been previously explored to address residual mechanical and microvascular deficiencies (6–8)). Unfortunately, therapeutic efficacy remains suboptimal due to the inability of those treatment modalities to provide oxygen to cardiac cells during the initial, irreversible stages of tissue damage that eventually lead to heart failure (9,10).

Previously, our group investigated a novel, photosynthetic therapy to rescue ischemic myocardium by direct injection of *Synechococcus elongatus*, a cyanobacterium, into the ischemic ventricle following a myocardial infarction (11). *S. elongatus* produces oxygen as a metabolic by-product of photosynthesis from carbon dioxide and water. Direct treatment with *S. elongatus* resulted in a biocompatible therapy that increased tissue oxygenation, improved left ventricular function, and enhanced cellular metabolism and function (11–13). Topical treatment also resulted in enhanced wound healing in a peripheral arterial disease model (14). Here, we sought to improve upon this technology by encapsulating *S. elongatus* into hydrogel microparticles (HMPs) in order to provide mechanical support to the cyanobacteria during injection, enhance therapeutic potential by adopting a minimally invasive approach, and enable broad clinical translation by packaging the live therapeutic in a biocompatible vessel.

HMPs or microgels have been widely studied for minimally invasive delivery of cells and/or biologics (15,16). HMPs can be fabricated into a variety of different shapes and sizes on the microscale and can be delivered in a suspension, as granular

* Corresponding author. Department of Cardiothoracic Surgery, Stanford University, Stanford, CA 94305, USA.
E-mail address: joswoo@stanford.edu (Y.-P.J. Woo).

1389-1723/$ – see front matter
https://doi.org/10.1016/j.jbiosc.2023.03.001

hydrogels, or as a composite network within a bulk hydrogel. Additionally, HMP systems are extremely modular, meaning that varying HMP compositions, sizes, and cargo can be combined in a multifunctional therapeutic approach (17). Cell encapsulation into HMPs is advantageous over direct cell injections because the cells are protected from the shear forces inflicted on them during the injection process, resulting in improved viability (18). Cell-laden HMPs have been explored in a variety of applications utilizing different polymeric components. Alginate HMPs in particular are attractive delivery vehicles due to their promising biocompatibility profile and ease of gelation (19,20). Previous studies investigated loading *S. elongatus*, or other photosynthetic microorganisms, into bioengineered constructs for tissue engineering and regeneration, organ preservation, wound healing, and cardiovascular disease (21–24). Yet, these scaffolds are not amenable to minimally invasive delivery. To address this shortcoming, we sought to encapsulate *S. elongatus* into alginate HMPs utilizing a simple T-junction microfluidic device, easily accessible to non-specialists in the field. Specifically, we found that encapsulation of *S. elongatus* and delivery of a *S. elongatus*-HMP suspension enhances microbial viability post-injection, further mitigates cellular apoptosis, and improves left ventricular function compared to direct *S. elongatus* injection. Furthermore, this approach yields homogenous HMPs with negligible impact to *S. elongatus* viability during the encapsulation and gelation process. These results suggest a promising delivery platform for photosynthetic treatment of ischemic tissue, potentially expanding the scope of oxygen-generating therapeutics.

MATERIALS AND METHODS

Elongatus culture *S. elongatus* culture and propagation protocol was published previously (11–14). Briefly, frozen *S. elongatus* vials (A14259, Life Technologies Corporation, Carlsbad, CA, USA) was transferred from the −80 °C freezer to thaw quickly in a 35 °C water bath without agitating the vial. In a baffled bottom flask with vented cap (4116–0125, ThermoFisher, Waltham, MA, USA), 30 mL of room temperature Gibco BG-11 cyanobacteria medium (A1379902, Life Technologies) was added, followed by the thawed cyanobacteria content from the vial. The culture was then placed on a rotating incubator (420, Thermo Electron Corporation, Waltham, MA, USA) at 34 °C and 125 rpm. Two 18-inch plant fluorescent light bulbs (F18T8 PL/AQ, General Electric, Boston, MA, USA) were placed on top of the incubator to allow for growth and photosynthesis. BG-11 medium was added to the culture every other day. The optical density of the stocks was measured using Spectronic Genesys 6 (Thermo Electron Corporation Instruments) at a wavelength of 750 nm. When the colony becomes oversaturated, the cultures were diluted with BG-11 media and split. Throughout the study, contamination checks were performed regularly by visual assessment under the microscopy and by culturing *S. elongatus* liquid on Luria broth agar to ensure no heterogeneous bacterial subpopulation growth.

Elongatus alginate HMP formation Alginate HMPs were fabricated based on a modified protocol published previously (20). All chemicals were procured from Sigma Aldrich unless otherwise specified. Alginate was dissolved at 2 wt% in BG-11 cyanobacteria media (A1379901, ThermoFisher). Calcium chloride (100 mM) and disodium-EDTA (100 mM) were each dissolved in BG-11 media. The calcium chloride solution was mixed with the disodium-EDTA solution at a 1:1 volume ratio and adjusted to a pH of 7 using sodium hydroxide resulting in a calcium-EDTA solution. The calcium-EDTA solution was added in equal volume to the alginate solution and mixed well, resulting in an alginate-calcium-EDTA complex. *S. elongatus* (7.7×10^8 cells/mL) harvested from the stock culture actively undergoing photosynthesis generating oxygen were then suspended into the alginate-calcium-EDTA complex and gently mixed, forming an *S. elongatus*-alginate-calcium-EDTA suspension. Fluorinated carbon oil (HFE7500) with 008-FluoroSurfactant (RAN Biotechnology, Beverly, MA, USA) was mixed with acetic acid (0.05 vol%) to generate the fluorinated oil mixture.

To create the emulsion, 5 mL of the fluorinated carbon oil mixture (oil phase) was added to a 5 mL syringe. The *S. elongatus*-alginate-calcium-EDTA complex (aqueous phase) was added to a 1 mL syringe. A T-junction microfluidic device was used similar to our previous work (25), with minor redesign for passive (valveless) operation using volumetric flow via syringe pumps. The device was fabricated via soft-lithography using PDMS polymer (RTV, Momentive, Niskayuna, NY, USA) (25). Both syringes were placed into separate syringe pumps, connected to the microfluidic device using ETFE tubing (Dolomite Microfluidics, Royston, UK), and set to a flow rate of 500 μL/h and 100 μL/h, respectively. The *S. elongatus*-alginate-calcium-EDTA suspension was emulsified into HMPs containing *S. elongatus*. Cross-linked *S. elongatus*-HMPs were collected in a BG-11 bath with 50 mM of calcium chloride and 10 wt% perfluoro-1-octanol (PFO; SynQuest Laboratories, Alachua, FL, USA). The bath was placed on a stir plate heated to 37 °C during *S. elongatus*-HMP collection. *S. elongatus*-HMPs were gently pipetted from the bath and washed three times with BG-11 and mild centrifugation. Images were acquired with a Zeiss confocal microscope with a 40× oil immersion objective (Zeiss, Oberkochen, Germany). These *S. elongatus*-HMPs were used immediately.

***In vitro* S. elongatus live/dead assay** After the emulsification process, *S. elongatus*-HMPs were transferred to an insulin syringe and injected through a 30-gauge needle. Similarly, *S. elongatus*, suspended in PBS, were injected through an insulin syringe with 30-gauge needle. Injections were performed in triplicate. The *S. elongatus* were then stained for viability using a live/dead kit (BacLight, ThermoFisher). Briefly, 3 μL of a solution consisting of equal parts 3.34 mM SYTO 9 dye and 20 mM propidium iodide was added per each milliliter of suspended bead solution. The beads were allowed to incubate at room temperature for 30 min to ensure adequate diffusion of the stains into the *S. elongatus*-HMPs. Images of the microgels were acquired using a Zeiss LSM 780× inverted confocal microscope and 40× oil immersion objective. Images were analyzed using ImageJ to determine the number of viable cells.

***In vitro* oxygen diffusion characterization** Each well in a 24-well plate was filled with 1.5 mL of PBS and allowed to equilibrate overnight in a hypoxia chamber glovebox (*X*3 Hypoxia Hood and Culture Combo from Xvivo System) set to 1% O_2, 5% CO_2, and 37 °C. Study groups were administered by first placing 0.4 μm transwells (Corning, Corning, NY, USA) into the wells in the 24-well plate. Each treatment was then added in triplicate via a 0.4 μm transwell to a well with equilibrated PBS and monitored over a 4-h period in the hypoxia chamber. The study groups were administered in 80 μL volumes as follows: PBS (control), 1×10^6 *S. elongatus* (therapeutic control), 20×10^3 HMPs (vehicle control), or 20×10^3 *S. elongatus*-HMPs per transwell. Oxygen content was measured using an Oxy Lite Pro O2 sensor (Oxford Optronix Ltd., Milton, UK) at the following time points: 0, 0.25, 0.5, 1, 2, 3, and 4 h. The sensor was placed mid-level in the well to measure oxygen content.

Culture of rat neonatal cardiomyocytes Neonatal rat cardiomyocytes (CMs) were isolated using the Pierce Primary Cardiomyocyte Isolation Kit (ThermoFisher) according to the manufacturer's instructions. Cardiac fibroblasts were removed from the cell population by pre-plating the cell culture for 2 h in primary DMEM (Fisher), supplemented with 10% FBS (Hyclone, Marlborough, MA, USA) and 1% penicillin-streptomycin (Fisher), before plating the CMs in 24-well plates at a density of 500,000 cells/well. Cells were incubated under 21% O_2, 5% CO_2, and 37 °C conditions and cell culture media was changed every 48 h.

Culture of human aortic smooth muscle cells Human aortic smooth muscle cells (AoSMCs) were purchased from Lonza (CC-2571) and grown in smooth muscle cell media (M231500, Fisher) with smooth muscle cell growth supplement (S00725, Fisher), 10% FBS (Hyclone) and 1% penicillin-streptomycin (Fisher). Cells were initially plated on 10 cm dishes with 10–15 mLs of media and grown until approximately 85% confluent, at which point they were passaged by trypsinization and seeded into 24-well plates. Cells were incubated under 21% O_2, 5% CO_2, and 37 °C conditions and cell culture media was changed every 48 h. Cells passage 8–9 were utilized for *in vitro* apoptosis assays described below.

***In vitro* apoptosis assay** Between 72 and 96-h after plating the cells, media was changed to serum free DMEM (Fisher) for approximately 12 h or overnight. The treatments were applied by first placing 0.4 μm transwells (Corning) in the 24-well plate with seeded CMs or AoSMCs followed by 80 L volume of one of four treatments: PBS (control), 1×10^6 *S. elongatus* (therapeutic control), 20×10^3 HMPs (vehicle control), or 20×10^3 *S. elongatus*-HMPs per transwell. Each group was investigated in triplicate. With the reported cell loading of roughly 50 *S. elongatus* per *S. elongatus*-HMP, 20×10^3 *S. elongatus*-HMPs equates to approximately 1×10^6 *S. elongatus* administered, for comparison purposes. The 24-well plate was transferred to a hypoxic chamber (*X*3 Hypoxia Hood and Culture Combo from Xvivo System) and cultured under hypoxic conditions (1% O_2, 5% CO_2, 37 °C) for 4 h. After incubation, an apoptosis assay was performed by adding Caspase-Glo 3/7 Assay System reagent (G8091, Promega, Madison, WI, USA) in an equal volume to the media present in the plate. Each plate was then placed in the normoxic incubator for 30 min according to the assay protocol. The contents of the 24-well plate were then mixed and transferred to a white 96-well plate and read on a luminescent plate reader (Synergy 2 BioTek Microplate reader, BioTek Instruments, Winooski, VT, USA) to quantify apoptosis.

Acute ischemia reperfusion and chronic ischemia reperfusion rat models All animal procedures were performed according to Stanford Animal Care and Use Committee approved protocols. For both the acute ischemia reperfusion (AIR) and chronic ischemia reperfusion (CIR) models, male Wistar rats ($n = 45$, 300–375 g) were sedated in an isoflurane chamber with 3% isoflurane (Fluriso, VetOne, Boise, ID, USA) at a flow rate of 1 L/min. Once anesthetized, a 16G

angiocatheter was used for endotracheal intubation and mechanical ventilation was initiated at 80 breaths/minute, a 3 mL tidal volume, PIP of 35 cmH2O, PEEP of 5, and a 33:66 I:E ratio (Hallowell EMC Pitt, Hallowell EMC, Pittsfield, MA, USA). Once on the ventilator, isoflurane was maintained at 1–2%.

In the AIR model, a median sternotomy was performed and an SPR-869 pressure-volume catheter (Millar) was introduced by cardiac puncture of the left ventricle with a 23-gauge needle. Baseline hemodynamics were then acquired. To induce myocardial ischemia, the left anterior descending artery (LAD) was temporarily occluded with a 6–0 polypropylene suture 2 mm below the level of the left atrial appendage. Immediately following LAD occlusion, animals were randomized ($n = 5$ per group) to receive intramyocardial injections of 80 μL volumes of either PBS, 1×10^6 *S. elongatus* suspended in PBS, 20×10^3 HMPs suspended in PBS, or 20×10^3 *S. elongatus*-HMPs suspended in PBS directly to the ischemic region. Continuous light exposure to the myocardium, aimed to primarily provide excellent exposure and visual for the operation powered by thePowerful 6 Watt LED Dual Gooseneck Illuminator (LED-6W, Amscope, Irvine, CA, USA) and the LED exam light (Berchtold Chromophare F300, Stryker, Kalamazoo, MI, USA) both at maximal intensity, was given throughout the duration of the surgery. For intramyocardial injections, a 30-gauge insulin syringe was used with the needle slightly bent to enter parallel to the endocardium and injections were administered in 4 spots within the infarct zone. Before injection, the plunger of the syringe was slightly drawn back to ensure that the needle was not intraventricular; wheal formation was visually checked to confirm an intramyocardial injection. Hemodynamics, such as end-systolic pressure volume relationship (ESPVR), were then serially acquired via left ventricular catheterization to obtain pressure-volume loops every 15 min for 45 min, the heart was reperfused, and then explanted for immunohistochemistry and histological analysis, as described in further detail below.

For the CIR model, a left thoracotomy was performed through the fourth intercostal space and the pericardium was opened to allow visualization of the left anterior descending artery (LAD). The LAD was temporarily occluded with a 6–0 prolene suture with the infarction confirmed by visual pallor change of the left ventricle. Immediately following LAD occlusion, animals were randomized ($n = 5$ per group) to receive intramyocardial injections of 80 μL volumes of either PBS, 1×10^6 *S. elongatus* suspended in PBS, 20×10^3 HMPs suspended in PBS, or 20×10^3 *S. elongatus*-HMPs suspended in PBS directly to the ischemic region. The LAD was occluded for 45 min, the suture was then removed, and the thoracotomy closed with 4–0 prolene suture. Isoflurane was weaned and the rats were extubated. At 4 weeks post-occlusion, animals underwent echocardiography to assess left ventricular (LV) function. All images were obtained using a VisualSonics Vevo 2100 (Fujifilm Visual Sonics Inc., Toronto, ON, Canada) digital imaging system with a MS250 transducer (13 MHz). Images were acquired at a mid-papillary level and apex level in the left ventricle parasternal short-axis B-mode and M-mode view. Image analysis was performed by a single, blinded investigator, and ejection fraction was calculated using the Vevo Lab software (Fujifilm Visual Sonics Inc.). After echocardiography, animals were euthanized and the hearts explanted for immunohistochemistry and histological analysis, as described in further detail below.

Five additional rats underwent a sham surgery in which a thoracotomy was performed, the heart exposed, and the pericardium opened. The ribs and skin were subsequently closed.

Animal randomization Animal cages were housed in a random order on the shelf. Physical randomization occurred before each operation. Echocardiography and analyses were done in a random order, with the individual being blinded to the treatment groups.

Statistical analysis All results are expressed as a mean ± standard deviation (s.d.). All *in vitro* studies were done in triplicate. Comparison between two groups were conducted by a two-tailed Student's *t*-test. One-way ANOVA with Turkey's multiple comparison test was used for comparison across multiple groups. Statistical significance was considered as $p < 0.05$.

RESULTS

Encapsulation of *S. elongatus* into alginate HMPs Using the T-junction microfluidic device, the cell-containing alginate-calcium-EDTA mixture was emulsified into monodisperse *S. elongatus*-HMPs (Fig. 1A–C). Cell-encapsulated alginate droplets were gelled post-device emulsification via a biocompatible pH-dependent Ca:EDTA chelation exchange in the collection bath (20). After gelation, the *S. elongatus*-HMPs were transferred to an aqueous bath, washed to remove residual acid and EDTA, and redispersed into BG-11 cell culture medium. The method is facile to perform by non-specialists and simple to translate, employing only two syringe pumps and a simple device (total cost: approximately $5000 per setup, $5.00 per reusable chip). HMP production is also a high throughput process. Microscopy images of *S. elongatus*-HMPs revealed high monodispersity (size 75.5 ± 5.6 μm) and homogenous distribution of *S. elongatus* (51.6 ± 14.1 cells/bead), exhibiting autofluorescence at 596 nm (Fig. 1D). Additionally, using a live/dead assay, we stained *S. elongatus* inside the *S. elongatus*-HMPs and found that 99.5% of the cells remain viable after the encapsulation and emulsification process.

Additionally, we evaluated the effectiveness of HMPs as cell delivery vehicles by injecting a suspension of *S. elongatus*-HMPs through a 30-gauge needle attached to a 1 mL syringe. The cellular viability of *S. elongatus* injected via an *S. elongatus*-HMP suspension was compared to the viability of *S. elongatus* injected in a suspension of PBS through a 30-gauge needle. Based on previous reports investigating the impact of direct cell injection on cellular viability, PBS injections were expected to greatly decrease cellular viability (26), but it was found that the viability of injected *S. elongatus* suspended in PBS resulted in an average viability of 93.3 ± 4%

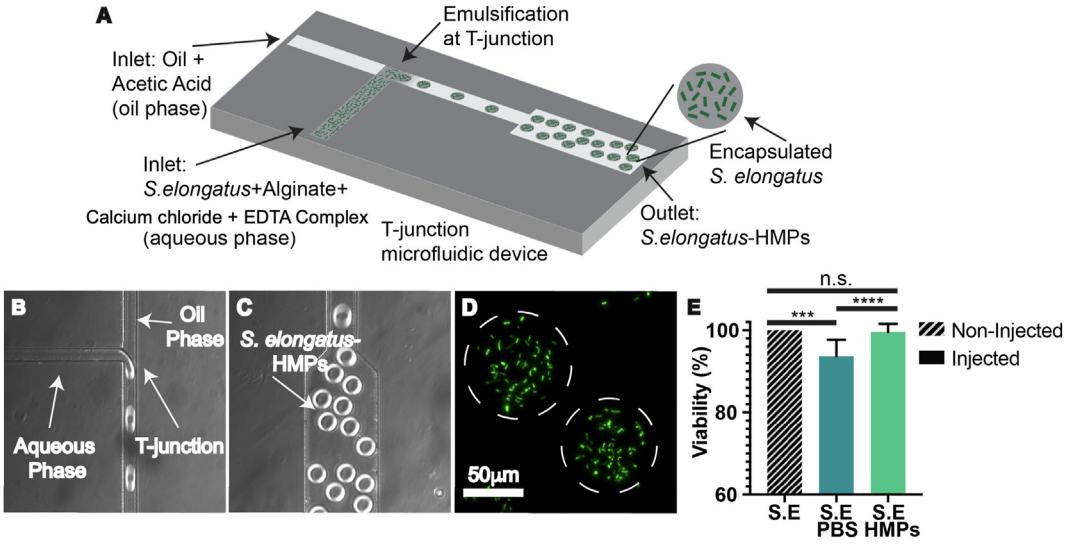

FIG. 1. (A) Schematic representation of T-junction microfluidic device for *S. elongatus*-HMP fabrication. (B) Zoomed in image of *S. elongatus*-HMP emulsification at the T-junction. (C) Zoomed in image of homogenous, monodispersed *S. elongatus*-HMPs. (D) Microscopy images of encapsulated *S. elongatus* in HMPs. (E) Percent viability of non-injected *S. elongatus* (S.E), injected *S. elongatus* in a suspension of PBS (S.E PBS) and injected *S. elongatus*-HMPs (S.E HMPs). Data presented as mean ± s.d. ($n \geq 10$). Statistical significance was determined against untreated controls ($^{***}p < 0.001$).

(reported as percent of cells alive). While significantly different from non-injected *S. elongatus* (100%, $p < 0.001$), this viability result suggests the resilient nature of *S. elongatus* and is consistent with previous literature reports on other robust cell types (27). When *S. elongatus*-HMPs were injected, however, the viability following injection increased significantly compared to the *S. elongatus* suspended in PBS group (99.5 ± 0.5%, $p < 0.0001$), with no significant difference from the non-injected *S. elongatus* control group (Fig. 1E). The increased viability in the *S. elongatus*-HMP group suggests an effective cell delivery vehicle that protects the cellular cargo from shear forces resulting from the injection process.

***S. elongatus*-HMPs oxygen diffusion mitigates cellular apoptosis under hypoxic conditions** To evaluate diffusion of oxygen from the *S. elongatus*-HMPs, oxygen generation was characterized by incubating *S. elongatus*-HMPs under hypoxic conditions (1% O_2, 5% CO_2, and 37 °C) and measuring the relative oxygen concentration compared to controls at set timepoints. In these studies, each well in a 24-well plate was filled with 1.5 mL of PBS and allowed to equilibrate overnight in a hypoxia chamber. Each treatment was then administered in triplicate and monitored over a 4-h period in the hypoxia chamber. The treatment groups were administered via transwells in 80 μL volumes as follows: PBS (control), 1×10^6 *S. elongatus* (therapeutic control), 20×10^3 HMPs (vehicle control), or 20×10^3 *S. elongatus*-HMPs. Oxygen content was measured at the following time points: 0, 0.25, 0.5, 1, 2, 3, and 4 h. After 1 h, *S. elongatus*-HMPs increased oxygen generation by 95% ($p < 0.01$) compared to untreated controls. After 4 h, *S. elongatus*-HMPs maintained the increased oxygen generation at 81% ($p < 0.01$) compared to the untreated controls (Fig. 2A). Oxygen generation from the *S. elongatus* PBS suspension and *S. elongatus*-HMPs was similar, suggesting adequate oxygen diffusion from the *S. elongatus*-HMPs (Fig. 2A).

To investigate the efficacy of *S. elongatus*-HMPs on cellular apoptosis under hypoxic conditions, rat neonatal CMs and AoSMCs were serum starved overnight and then cultured under hypoxic conditions for 4 h while undergoing treatment. Cells were treated with either PBS, *S. elongatus*, HMPs, or *S. elongatus*-HMPs as previously described. CMs and AoSMCs treated with *S. elongatus*-HMPs exhibited a 51% and 32% decrease in apoptosis, respectively, compared to the untreated control (Fig. 2B and C, $p < 0.01$). Cellular apoptosis did not significantly differ between cells treated with *S. elongatus* and *S. elongatus*-HMPs (p-value = 0.8345), suggesting that *S. elongatus* and *S. elongatus*-HMPs are similarly effective.

***S. elongatus*-HMPs improve left ventricular function during AIR and CIR models** We explored the immediate functional effects of *S. elongatus*-HMPs to determine whether enhanced tissue oxygenation in combination with mechanical support for the *S. elongatus* during injection would improve cardiac function compared to control groups (Fig. 3A). The AIR studies were performed using a left ventricle pressure-volume catheter for hemodynamic assessment at baseline and 45 min after treatment intervention immediately following reperfusion. Immediately following LAD occlusion, rats were randomized to receive the following treatments injected in 80 μL volumes as previously described: PBS, *S. elongatus*, HMPs, and *S. elongatus*-HMPs. ESPVR measurements taken after 45 min of ischemia were compared to ESPVR measurements taken at baseline to understand the change in ventricular contractility with or without treatment. After 45 min of ischemia, *S. elongatus*-HMP treated animals exhibited preserved ESPVR relative to baseline of 0.79 ± 0.04 vs 0.55 ± 0.08 in the untreated control group ($p < 0.001$) (Fig. 3B).

To investigate the long-term benefits of *S. elongatus*-HMPs, a CIR study was conducted in which animals were survived for 4 weeks and underwent echocardiography to assess left ventricular function. Echocardiographic assessment of cardiac function revealed significant functional benefits in the *S. elongatus*-HMP treated animals compared to control groups. At 4 weeks following the ischemia reperfusion injury, ejection fraction was significantly improved compared with that of the PBS group (*S. elongatus*-HMP 74.2 ± 3.9%; PBS, 53.1 + 8.0% $p < 0.001$), the HMP vehicle control group (58.5 + 3.6% $p < 0.001$), and the *S. elongatus* therapeutic control group (66.5 + 2.5% $p < 0.01$) (Fig. 3C).

DISCUSSION

The present study demonstrates a new method of delivery for a biocompatible photosynthetic therapy for myocardial ischemia. While *S. elongatus* utilizes light to convert H_2O and CO_2 into glucose and O_2, the HMPs protect the cellular integrity and viability of the *S. elongatus* cells during therapeutic injection. This approach extends our previous approach of direct cell delivery and offers significant advantages for clinical translation and therapeutic efficiency; as compared to direct cell delivery, our method provides mechanical support to the *S. elongatus,* resulting in improved therapeutic benefit to the ischemic tissue as well as minimally invasive delivery. The data show that alginate HMPs can serve as an effective carrier of *S. elongatus* and directly deliver oxygen to the ischemic myocardium following ischemic insult. This *S. elongatus*-

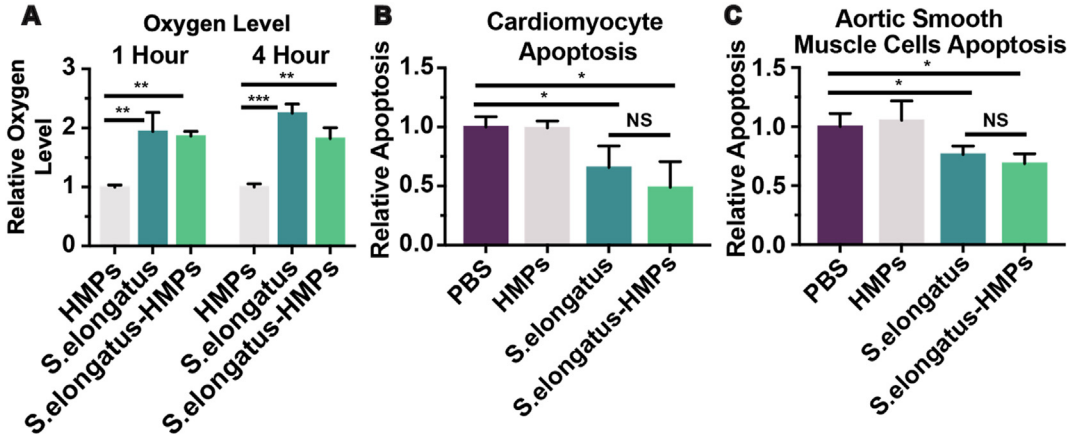

FIG. 2. (A) Oxygen generation data relative to the PBS control group at 1 h and 4 h timepoints. (B) *In vivo* efficacy of *S. elongatus*-HMPs on rat neonatal cardiomyocytes (CMs). (C) *In vivo* efficacy of *S. elongatus*-HMPs on human aortic smooth muscle cells (AoSMCs). Data presented as mean ± s.d. (n = 3). Statistical significance was determined against untreated controls ($^*p < 0.05$, $^{**}p < 0.01$, $^{***}p < 0.001$).

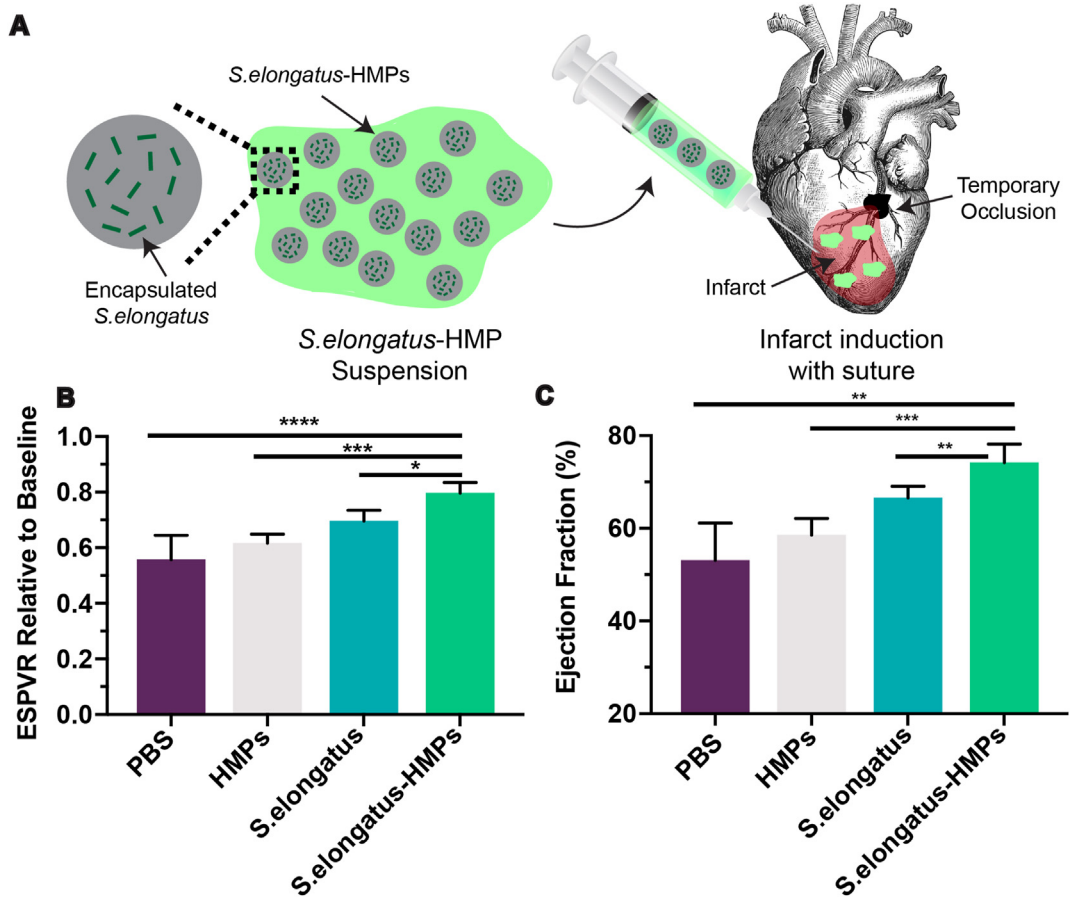

FIG. 3. (A) Schematic illustration of *S. elongatus* encapsulated into alginate hydrogel microparticles (*S. elongatus*-HMPs) and delivery to ischemic myocardial tissue, whereby ischemia was induced via a temporary occlusion of the left anterior descending artery (LAD). (B) *In vivo* efficacy of *S. elongatus*-HMPs on left ventricular function following acute myocardial ischemia. End-systolic pressure volume relationship (ESPVR) values taken following 45 min of ischemia and treatment were compared to the ESPVR values taken at baseline for each animal resulting in the retained ESPVR values reported in the graph. (C) *In vivo* efficacy of *S. elongatus*-HMPs on ejection fraction 4 weeks following ischemia reperfusion. Data presented as mean ± s.d. (n = 5). Statistical significance was determined against untreated controls ($^{*}p < 0.05$, $^{**}p < 0.01$, $^{***}p < 0.001$).

HMP treatment resulted in simple oxygen diffusion through the HMPs, mitigated cellular apoptosis, and improved left ventricular function.

The photosynthetic oxygen delivery system is based on a simple T-junction microfluidic platform allowing for facile droplet formation. This delivery system is advantageous compared to other HMP fabrication methods because of the rapid crosslinking mechanism (< 2 min) and robust, high-throughput method of gel formation. Our system is inexpensive (< $5000), straightforward to operate by non-specialists in the field, and simple to extend into existing commercial vendors (e.g., Dolomite Microfluidics) for widespread use. Gels made from our method are monodisperse and exhibit excellent cellular loading with consistent high-yield per microparticle. Most importantly, *S. elongatus* cells remain viable after the encapsulation/emulsification process and injection through a 30-gauge needle suggesting the biocompatible nature of this fabrication technique with *S. elongatus* encapsulation.

Our *in vitro* studies demonstrate that *S. elongatus*-HMPs retain the ability to directly deliver oxygen to CMs and AoSMCs leading to significantly reduced apoptosis under ischemic conditions. Previous studies have shown that extremely low oxygen conditions (< 1%) in infarcted hearts leads to irreversible cell death (28). We mimicked those conditions in our *in vitro* studies utilizing a hypoxia glove box set with atmospheric conditions set to 1% O_2. In this highly regulated hypoxia chamber, we showed continuous oxygen release from the *S. elongatus*-HMPs for at least 4 h. The therapeutic benefit of continuous oxygen release from the *S. elongatus*-HMPs was confirmed by the ability of the photosynthetic system to enhance the viability of CMs and AoSMCs after 4 h of culture in the hypoxia chamber. The enhanced viability and reduction in apoptosis following treatment with *S. elongatus*-HMPs also builds upon our previously published study investigating the therapeutic impact of *S. elongatus* on *in vitro* cardiomyocyte function. Our previous work demonstrated that *S. elongatus* therapy improves cardiomyocyte proliferation under hypoxic conditions. Our *in vitro* apoptosis study demonstrates *S. elongatus* and *S. elongatus*-HMPs to be similarly effective in reducing apoptosis under hypoxic conditions suggesting the potential of *S. elongatus*-HMPs to also improve cardiomyocyte proliferation and function. Finally, *in vivo* treatment with *S. elongatus*-HMPs, in both short-term and long-term ischemia models, resulted in improved cardiac function.

Alginate HMPs are an attractive *S. elongatus* delivery vehicle for the treatment of myocardial infarction due to their inherently tunable nature. The degree of crosslinking and delivery mechanism (i.e., HMPs delivered as a suspension, concentrated as a granular hydrogel, or embedded into a bulk hydrogel) can be easily modified to tune the network stiffness, oxygen diffusion profile, and amenability for minimally-invasive delivery techniques. Additionally, HMPs can be fabricated with varying composition, size, and contents, suggesting the ability to create a platform for a combinatorial treatment with oxygen delivery (17). Since the HMPs were delivered intramyocardially, there was no concern of coronary artery occlusion. Synergistic growth factors or cytokines could be used in conjunction with photosynthetic oxygen delivery to

provide a wholistic approach to the microvascular perfusion deficits that contribute to eventual heart failure (29–31). As a future direction, further studies of different HMP delivery systems should be investigated to understand the complete potential of *S. elongatus*-HMPs as a photosynthetic oxygen delivery system to the ischemic myocardium. Previous studies have also demonstrated the benefits of cell encapsulation over direct cell injection due to the protection of cellular cargo and the reduction in cellular regurgitation following injection (18). Furthermore, numerous studies have demonstrated fewer than 5% of injected cells persisting at the site of injection within days of transplantation and hydrogels microparticle cell carriers have been shown to improve retention and localization of the injected therapeutic cargo (32). Further studies investigating the extent of localized oxygen delivery, HMP stability and degradation at the injection site, *S. elongatus* retention and proliferation *in vivo*, and protection from local inflammatory environment would further support the resulting functional benefits shown in this work. Alginate specifically has been extensively studied in the literature and is an attractive polymer for HMP delivery systems due to the favorable biocompatibility profile of alginate materials (33,34). While alginate is inherently non-degradable in mammals and slowly dissolves over time by the release of the divalent ions cross-linking the hydrogel into the surrounding environment, alginate chains can be modified and undergo partial oxidation to allow for degradation under physiological conditions (19,35). Incorporating partially oxidized alginate chains and investigating the tunable degradation of alginate should be incorporated into future studies investigating this platform.

One limitation of this study is the need for a light source following administration of the photosynthetic therapy which requires an invasive surgical operation. However, a new chlorophyll pigment, chlorophyll f, has been previously discovered in a different strain of cyanobacteria (36) and absorbs light in the infrared spectrum. This chlorophyll f strain could allow for transcutaneous delivery of light instead of requiring open incision for access to light and further enhance the therapeutic potential of this therapeutic. Additionally, because HMPs are amenable to minimally invasive delivery, chlorophyll f strains of cyanobacteria could potentially be delivered via catheter in conjunction with the transcutaneous light access that the chlorophyll f strain would allow. Thus, future studies encapsulating a far-red cyanobacteria would be a potential solution to the limitation regarding light access and a promising step towards clinical translation. Future studies should also investigate the impact of alginate HMPs on cardiac tissue structure. For example, investigating cardiomyocyte death following administration of the alginate HMPs will help better understand the beneficial impact of this therapeutic approach.

In summary, we have developed a novel, photosynthetic oxygen delivery system that has shown promising therapeutic efficacy *in vitro* and *in vivo*. This treatment approach has the potential to treat ischemic tissue during a period of absent blood flow and be delivered to ischemic hearts during coronary revascularization following myocardial infarction. Overall, our *S. elongatus*-HMP oxygen delivery system establishes a proof of concept for a minimally invasive technology for myocardial ischemia.

ACKNOWLEDGMENTS

This study was supported, in part, by the National Institutes of Health grant R01 HL089315-01 (YJW), Stanford Bio-X Interdisciplinary Seed Grant (EAA and YJW), National Graduate Research Fellowship (LMS and GAR), American Heart Association Predoctoral Fellowship (LMS), American Heart Association Postdoctoral Fellowship (HW and MJP), ChemH Chemical Biology Interface T32 Training Grant (KKB), and SIGF/BIOX (LMS). P.M.F. is a Chan Zuckerberg Biohub Investigator. The authors have no conflicts of interest to disclose. L.M.S., J.M.F., M.J.P., G.A.R., K.B., P.F., E.A.A. and Y.J.W., designed experiments and microfluidic system; L.M.S., J.M.F., H.J.L., K.P.T., conducted experiments; L.M.S., H.W., E.A.A., and Y.J.W, analyzed data; and L.M.S., J.M.F., H.J.L, Y.Z., H.W., E.A.A., and Y.J.W wrote paper.

References

1. **Mozaffarian, D., Benjamin, E. J., Go, A. S., Arnett, D. K., Blaha, M. J., Cushman, M., Das, SR, de Ferranti, S, Després, JP, Fullerton, HJ, and other 34 authors:** Executive summary: heart disease and stroke statistics–2016 update: a report from the American heart association, Circulation, **133**, 447–454 (2016).
2. **Benjamin, E. J., Muntner, P., Alonso, A., Bittencourt, M. S., Callaway, C. W., Carson, A. P., Chamberlain, A. M., Chang, A. R., Cheng, S., Das, S. R., and other 38 authors:** Heart disease and stroke statistics-2019 update: a report from the American heart association, Circulation, **139**, e56–e528 (2019).
3. **Heidenreich, P. A., Trogdon, J. G., Khavjou, O. A., Butler, J., Dracup, K., Ezekowitz, M. D., Finkelstein, EA, Hong, Y, Johnston, SC, Khera, A, and other 18 authors:** Forecasting the future of cardiovascular disease in the United States: a policy statement from the American Heart Association, Circulation, **123**, 933–944 (2011).
4. **Reddy, K., Khaliq, A., and Henning, R. J.:** Recent advances in the diagnosis and treatment of acute myocardial infarction,, World J. Cardiol., **7**, 243–276 (2015).
5. **Araszkiewicz, A., Grajek, S., Lesiak, M., Prech, M., Pyda, M., Janus, M., and Cieslinski, A.:** Effect of impaired myocardial reperfusion on left ventricular remodeling in patients with anterior wall acute myocardial infarction treated with primary coronary intervention, Am. J. Cardiol., **98**, 725–728 (2006).
6. **Franco, S. D., Amarelli, C., Montalto, A., Loforte, A., and Musumeci, F.:** Biomaterials and heart recovery: cardiac repair, regeneration and healing in the MCS era: a state of the "heart,", J. Thorac. Dis., **10**, S2346–S2362 (2018).
7. **Lam, M. T. and Wu, J. C.:** Biomaterial applications in cardiovascular tissue repair and regeneration, Expert Rev. Cardiovasc. Ther., **10**, 1039–1049 (2012).
8. **Stapleton, L., Zhu, Y., Woo, Y. J., and Appel, E.:** Engineered biomaterials for heart disease, Curr. Opin. Biotechnol., **66**, 246–254 (2020).
9. **Lister, Z., Rayner, K. J., and Suuronen, E. J.:** How biomaterials can influence various cell types in the repair and regeneration of the heart after myocardial infarction, Front. Bioeng. Biotechnol., **4**, 62 (2016).
10. **Pascual-Gil, S., Garbayo, E., Díaz-Herráez, P., Prosper, F., and Blanco-Prieto, M. J.:** Heart regeneration after myocardial infarction using synthetic biomaterials, J. Control. Release, **203**, 23–38 (2015).
11. **Cohen, J. E., Goldstone, A. B., Paulsen, M. J., Shudo, Y., Steele, A. N., Edwards, B. B., Patel, J. B., MacArthur, J. W., Jr., Hopkins, M. S., Burnett, C. E., and other 13 authors:** An innovative biologic system for photon-powered myocardium in the ischemic heart, Sci. Adv., **3**, e1603078 (2017).
12. **Wang, H., Wu, M., and Woo, Y. J.:** Photosynthetic symbiotic therapy, Aging, **11**, 843–844 (2019).
13. **Williams, K. M., Wang, H., Paulsen, M. J., Thakore, A. D., Rieck, M., Lucian, H. J., Grady, F, Hironaka, C. E., Chien, A. J., Farry, J. M., and other 7 authors:** Safety of photosynthetic Synechococcus elongatus for in vivo cyanobacteria-mammalian symbiotic therapeutics, Microb. Biotechnol., **13**, 1780–1792 (2020).
14. **Zhu, Y., Jung, J., Anilkumar, S., Ethiraj, S., Madira, S., Tran, N. A., Mullis, D. M., Casey, K. M., Walsh, S. K., Stark, C. J., and other 4 authors:** A novel photosynthetic biologic topical gel for enhanced localized hyperoxygenation augments wound healing in peripheral artery disease, Sci. Rep., **12**, 10028 (2022).
15. **Daly, A. C., Riley, L., Segura, T., and Burdick, J. A.:** Hydrogel microparticles for biomedical applications, Nat. Rev. Mater., **5**, 20–43 (2020).
16. **Li, W., Zhang, L., Ge, X., Xu, B., Zhang, W., Qu, L., Choi, C. H., Xu, J., Zhang, A., Lee, H., and Weitz, D. A.:** Microfluidic fabrication of microparticles for biomedical applications, Chem. Soc. Rev., **47**, 5646–5683 (2018).
17. **Mealy, J. E., Chung, J. J., Jeong, H. H., Issadore, D., Lee, D., Atluri, P., and Burdick, J. A.:** Injectable granular hydrogels with multifunctional properties for biomedical applications, Adv. Mater., **30**, e1705912 (2018).
18. **Foster, A. A., Marquardt, L. M., and Heilshorn, S. C.:** The diverse roles of hydrogel mechanics in injectable stem cell transplantation, Curr. Opin. Chem. Eng., **15**, 15–23 (2017).
19. **Lee, K. Y. and Mooney, D. J.:** Alginate: properties and biomedical applications, Prog. Polym. Sci., **37**, 106–126 (2012).
20. **Utech, S., Prodanovic, R., Mao, A. S., Ostafe, R., Mooney, D. J., and Weitz, D. A.:** Microfluidic generation of monodisperse, structurally homogeneous alginate microgels for cell encapsulation and 3D cell culture, Adv. Healthc. Mater., **4**, 1628–1633 (2015).
21. **Chávez, M. N., Schenck, T. L., Hopfner, U., Centeno-Cerdas, C., Somlai-Schweiger, I., Schwarz, C., Machens, H. G., Heikenwalder, M., Bono, M. R., Allende, M. L., Nickelsen, J., and Egaña, J. T.:** Towards autotrophic tissue

engineering: Photosynthetic gene therapy for regeneration, Biomaterials, **75**, 25–36 (2016).
22. **Haraguchi, Y., Kagawa, Y., Sakaguchi, K., Matsuura, K., Shimizu, T., and Okano, T.:** Thicker three-dimensional tissue from a "symbiotic recycling system" combining mammalian cells and algae, Sci. Rep., **7**, 41594 (2017).
23. **Hopfner, U., Schenck, T. L., Chávez, M. N., Machens, H. G., Bohne, A. V., Nickelsen, J., Giunta, R. E., and Egaña, J. T.:** Development of photosynthetic biomaterials for in vitro tissue engineering, Acta Biomater., **10**, 2712–2717 (2014).
24. **Schenck, T. L., Hopfner, U., Chávez, M. N., Machens, H. G., Somlai-Schweiger, I., Giunta, R. E., Bohne, A. V., Nickelsen, J., Allende, M. L., and Egaña, J. T.:** Photosynthetic biomaterials: a pathway towards autotrophic tissue engineering, Acta Biomater., **15**, 39–47 (2015).
25. **Brower, K. K., White, A. K., and Fordyce, P. M.:** Multi-step variable height photolithography for valved multilayer microfluidic devices, J. Vis. Exp., **119**, e55276 (2017).
26. **Aguado, B. A., Mulyasasmita, W., Su, J., Lampe, K. J., and Heilshorn, S. C.:** Improving viability of stem cells during syringe needle flow through the design of hydrogel cell carriers, Tissue Eng., **18**, 806–815 (2012).
27. **Hernandez, H., Grosskopf, A. K., Stapleton, L. M., Agmon, G., and Appel, E. A.:** Non-Newtonian polymer–nanoparticle hydrogels enhance cell viability during injection, Macromol. Biosci., **19**, 1800275 (2018).
28. **Xu, Y., Fu, M., Li, Z., Fan, Z., Li, X., Liu, Y., Anderson, P. M., Xie, X., Liu, Z., and Guan, J.:** A prosurvival and proangiogenic stem cell delivery system to promote ischemic limb regeneration, Acta Biomater., **31**, 99–113 (2016).
29. **Cohen, J. E., Purcell, B. P., MacArthur, J. W., Mu, A., Shudo, Y., Patel, J. B., Brusalis, C. M., Trubelja, A., Fairman, A. S., Edwards, B. B., and other 7 authors:** A bioengineered hydrogel system enables targeted and sustained intramyocardial delivery of neuregulin, activating the cardiomyocyte cell cycle and enhancing ventricular function in a murine model of ischemic cardiomyopathy, Circ. Heart Fail., **7**, 619–626 (2014).
30. **Wang, H., Wisneski, A., Paulsen, M. J., Imbrie-Moore, A., Wang, Z., Xuan, Y., Hernandez, H. L., Lucian, H. J., Eskandari, A., Thakore, A. D., and other 9 authors:** Bioengineered analog of stromal cell-derived factor 1α preserves the biaxial mechanical properties of native myocardium after infarction, J. Mech. Behav. Biomed. Mater., **96**, 165–171 (2019).
31. **Steele, A. N., Cai, L., Truong, V. N., Edwards, B. B., Goldstone, A. B., Eskandari, A., Mitchell, A. C., Marquardt, L. M., Foster, A. A., Cochran, J. R., Heilshorn, S. C., and Woo, Y. J.:** A novel protein-engineered hepatocyte growth factor analog released via a shear-thinning injectable hydrogel enhances post-infarction ventricular function, Biotechnol. Bioeng., **114**, 2379–2389 (2017).
32. **Amer, M. H., Rose, F. R., Shakesheff, K. M., Modo, M., and White, L. J.:** Translational considerations in injectable cell-based therapeutics for neurological applications: concepts, progress and challenges, NPJ Regen. Med., **2**, 23 (2017).
33. **Liberski, A., Latif, N., Raynaud, C., Bollensdorff, C., and Yacoub, M.:** Alginate for cardiac regeneration: from seaweed to clinical trials, Glob. Cardiol. Sci. Pract., **2016**, e201604 (2016).
34. **Ruvinov, E. and Cohen, S.:** Alginate biomaterial for the treatment of myocardial infarction: progress, translational strategies, and clinical outlook: from ocean algae to patient bedside, Adv. Drug Deliv. Rev., **96**, 54–76 (2016).
35. **Cattelan, G., Guerrero Gerbolés, A., Foresti, R., Pramstaller, P. P., Rossini, A., Miragoli, M., and Caffarra Malvezzi, C.:** Alginate formulations: current developments in the race for hydrogel-based cardiac regeneration, Front. Bioeng. Biotechnol., **8**, 414 (2020).
36. **Chen, M., Schliep, M., Willows, R. D., Cai, Z. L., Neilan, B. A., and Scheer, H.:** A red-shifted chlorophyll, Science, **329**, 1318–1319 (2010).